Measuring Binding Kinetics of Ligands with Tethered Receptors by Fluorescence Polarization and Total Internal Reflection Fluorescence

ARTICLE *in* ANALYTICAL CHEMISTRY · APRIL 2010

Impact Factor: 5.64 · DOI: 10.1021/ac1002245 · Source: PubMed

2 AUTHORS, INCLUDING:

Nh Cheung
Hong Kong Baptist University
53 PUBLICATIONS **937** CITATIONS

SEE PROFILE

Anal. Chem. **2010,** *82,* 3819–3825

Measuring Binding Kinetics of Ligands with Tethered Receptors by Fluorescence Polarization and Total Internal Reflection Fluorescence

Ka-Cheung Kwok and Nai-Ho Cheung*

Department of Physics, Hong Kong Baptist University, Hong Kong, China

Binding kinetics of nuclear receptors and their specific ligands was measured using polarization anisotropy complemented with total internal reflection fluorescence. Binding affinities of tethered full length human estrogen receptor alpha (ERα) with 17β-estradiol, diethylstilbestrol, raloxifene, 4-hydroxytamoxifen, tamoxifen, and genistein were measured to be 100 (as reference), 100, 35, 21, 8, and 1.5, respectively. They agreed with published results. For the first time, rate constants were measured, and off rates were 1.5, 1.5, 1.3, 1.6, 1.7, and 2.3×10^{-3} s^{-1} while on rates were 11, 10, 3.3, 2.4, 1.0, and 0.26×10^{5} $M^{-1}s^{-1}$, respectively. For the antiestrogen drugs, their comparable off-rates correlated well with their equally similar potency. Eleven ginsenosides were screened as potential ligands. None were found to bind to ERα, but Rb1(S) and 20(S)-Rg3 were shown to bind to peroxisome proliferator-activated receptor gamma. The latter finding corroborated strongly with the therapeutic effects of ginsenosides on diabetic mice observed in a separate study. Our method would complement surface plasmon resonance assay for small ligands in the mass range of tens to hundreds of Daltons.

Numerous physiological processes are mediated by receptor−ligand interactions. One example is the binding of estrogens with their receptors. This can lead to the proliferation of cancerous mammary cells. Consequently, antagonist drugs were developed which could compete with endogenous hormones for the receptor site.[1] Another example is the binding of hormone receptors with certain environmental contaminants. This can disrupt endocrine functions to cause health problems.[2] One therefore wants to measure the binding between receptors and ligands, be it for lead optimization in drug discovery, or for large scale screening of endocrine disruptors. Specifically, equilibrium and kinetic rate constants of receptor−ligand interaction are to be measured *in vitro*.[3,4]

These binding constants may be measured by radioisotope or optical assays.[5] For safety reasons, the latter is preferred. In these studies, the reagents are mixed in solution and kinetics is studied by stopped-flow. More recently, however, tethered receptors in flow cells are used because this format uses less chemicals, allows reagent injection amidst reactions, and can be parallel-processed like microarrays for high throughput screening. Examples of this format include the widely adopted surface plasmon resonance (SPR) and the newer reflectance interferometry.[6,7] They detect optical changes due to the increase in mass. No analyte labeling is necessary. For small ligands like estrogens (272 D), nonetheless, the minute mass increase can evade detection. That probably explains why only leading SPR experts had measured estrogen binding kinetics.[8] If still smaller ligands are to be studied, as in fragment-based drug discovery,[9] SPR will be seriously handicapped.

Fluorescence based techniques can be more sensitive. For example, total-internal-reflection fluorescence (TIRF) can detect single fluorophores.[10] It has been used by itself,[11] and in combination with fluorescence correlation spectroscopy,[12] and photobleaching recovery,[13] to measure affinities and kinetics of receptor−ligand interactions. We have previously used TIRF to measure the adsorption kinetics of single molecules of bovine serum albumin.[14,15] Another useful technique is fluorescence polarization (FP). It detects the fluorescence anisotropy of small fluorescent ligands whose tumbling is slowed when they bind to protein receptors.[10] Although dye labeling is a concern in these

* To whom correspondence should be addressed. E-mail: nhcheung@hkbu.edu.hk.

(1) Jordan, V. C. *Cancer* **1992**, *70*, 977–982.
(2) Current Status of Test Methods for Detecting Endocrine Disruptors: In Vitro Estrogen Receptor Binding Assays; NIH Publication 03−4504; National Institutes of Health, October 2002.
(3) Copeland, R. A. *Evaluation of Enzyme Inhibitors in Drug Discovery*; Wiley Interscience: Hoboken, NJ, 2005.
(4) Tummino, J. P.; Copeland, R. A. *Biochemistry* **2008**, *47*, 5481–5492.
(5) *Protein-Ligand Interactions, Methods and Applications*; Nienhaus, G. U., Ed.; Humana Press: Totowa, NJ, 2005.
(6) Rich, R. L.; Myszka, D. G. *Drug Discovery Today: Technol.* **2004**, *1*, 301–308.
(7) Gavutis, M.; Lata, S.; Lamken, P.; Muller, P.; Piehler, J. *Biophys. J.* **2005**, *88*, 4289–4302.
(8) Rich, R. L.; Hoth, L. R.; Geoghegan, K. F.; Brown, T. A.; LeMotte, P. K.; Simons, S. P.; Hensley, P.; Myszka, D. G. *Proc. Natl. Acad. Sci. U.S.A.* **2002**, *99*, 8562–8567.
(9) Hopkins, A. L.; Groom, C. R.; Alex, A. *Drug Discovery Today* **2004**, *9*, 430–431.
(10) Lakowicz, J. R. *Principles of Fluorescence Spectroscopy,* 3rd ed.; Springer: New York, 2006.
(11) Schmid, E. L.; Tairi, A.-P.; Hovius, R.; Vogel, H. *Anal. Chem.* **1998**, *70*, 1331–1338.
(12) Lieto, A. M.; Cush, R. C.; Thompson, N. L. *Biophys. J.* **2003**, *85*, 3294–3302.
(13) Hsieh, H. V.; Thompson, N. L. *Biochemistry* **1995**, *34*, 12481–12488.
(14) Yeung, K. M.; Lu, Z. J.; Cheung, N. H. *Colloids Surf., B* **2009**, *69*, 246–250.
(15) Kwok, K. C.; Yeung, K. M.; Cheung, N. H. *Langmuir* **2007**, *23*, 1948–1952.

10.1021/ac1002245
Published on Web 04/13/2010

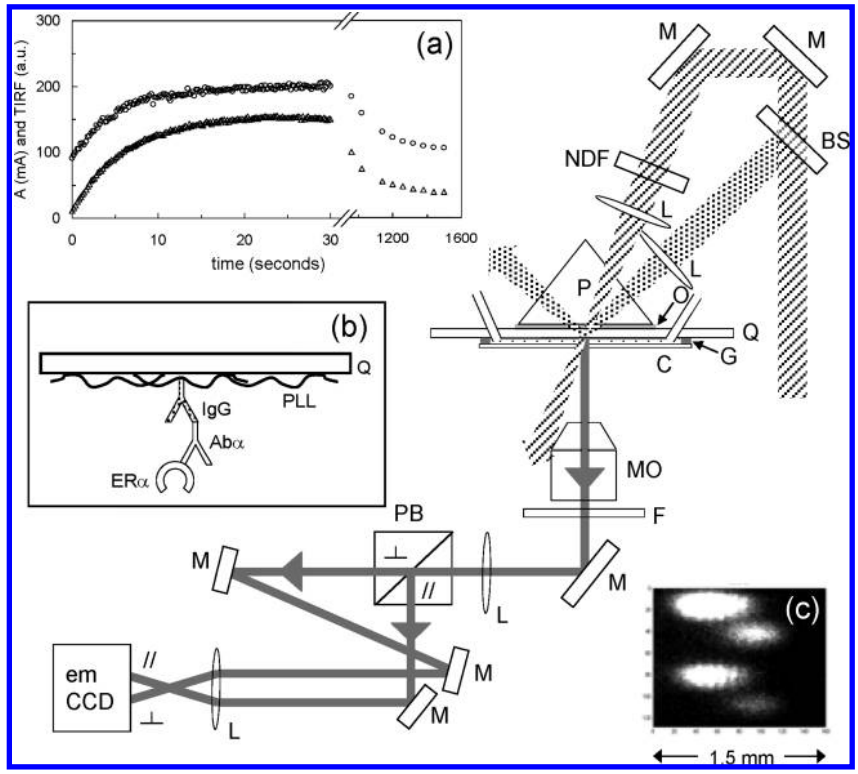

Figure 1. Experimental setup of the FP-TIRF system: BS, beam splitter; C, coverglass; emCCD, electron-multiplied charge-coupled device; F, band filter; G, vacuum grease; L, lens; M, mirror; MO, microscope objective; NDF, neutral density filter; O, immersion oil; P, prism; and Q, quartz slide. (a) Polarization anisotropy *A* and TIRF signal. A 2 nM sample of F was injected at $t = 0$, and 20 μM 4OHT was injected at $t = 900$ s while *A* (○) and TIRF signal (△) were captured simultaneously. (b) ERα tethering scheme: Q, quartz; PLL, poly-L-lysine; IgG, primary antibody; Abα, secondary antibody; ERα, estrogen receptor α. (c) Typical image. The four spots from top to bottom were BF∥, TIRF∥, BF⊥, and TIRF⊥. Dimensions of the corresponding object were indicated.

fluorescence measurements, one may detect dark ligands by tracking their displacement of bright reporters.[16,17]

FP has been widely used to measure receptor−ligand interactions at equilibrium,[2] as well as binding kinetics in stopped-flow mixing.[18,19] As far as we know, it has not been used to measure binding kinetics of tethered receptors. Here, we report the design and implementation of an FP-TIRF system for measuring the binding kinetics of small ligands with tethered receptors. We will show that our method was reliable, and it complemented SPR in many ways. We report, for the first time, the rate constants of the binding of full-length human estrogen receptor alpha (ERα) with its standard ligands. Our measured affinities agreed with published results. The antiestrogen drugs that we studied were shown to have dissimilar affinities. Yet their comparable off-rates correlated with their equally similar potency in reducing breast cancer. We also screened ginsenosides for binding with ERα and peroxisome proliferator-activated receptor gamma (PPARγ). High affinity ligands were identified, which corroborated the therapeutic effects of ginsenosides on diabetic mice demonstrated in a separate study.

EXPERIMENTAL SECTION

Apparatus. The FP-TIRF system is shown schematically in Figure 1. It was built around an inverted microscope. The sample cell was made from a quartz slide Q coated with receptor on the underside, filled with buffer, sandwiched with a cover glass C, and sealed with vacuum grease G. Liquid inlet and outlet were inserted from the top. The cell was clamped onto the traveling stage and coupled via immersion oil O to a prism P that was fixed relative to the microscope stand. The cell could freely translate without moving the prism. A 473-nm laser beam was split two ways with a beam splitter BS. One beam was focused with lens L and incident through the prism on the quartz−water interface at 70° and was totally reflected internally to produce the TIRF signal. The evanescent layer was about 100 nm thick.[15] The other beam was steered with mirrors M and incident through the prism on the quartz−water interface at 41° to produce the bulk fluorescence BF signal. The incident laser beam was TE polarized (s-wave) and the laser power of the two arms was balanced with a neutral density filter NDF. Fluorescence signal was collected by a 10× NA 0.25 microscope objective MO, band-filtered F, and directed through a polarizing beamsplitter PB. The dual images were captured with an electron-multiplied CCD (emCCD). Part c is a typical image. The four spots from top to bottom were BF∥, TIRF∥, BF⊥, and TIRF⊥. Dimensions of the corresponding object were indicated. Further instrumentation details can be found in the Supporting Information.

Receptor Tethering. The receptors ERα were tethered on the quartz slide and the cover glass. The multilayer tethering

(16) Thoma, N.; Goody, R. S. In *Kinetic Analysis of Macromolecules*; Johnson, K. A., Ed.; Oxford University Press: Oxford, 2003; pp 153−170.
(17) Motulsky, H. J.; Mahan, L. C. *Mol. Pharmacol.* **1984**, *25*, 1–9.
(18) Wilkinson, J. C.; Stein, R. A.; Guyer, C. A.; Beechem, J. M.; Staros, J. V. *Biochemistry* **2001**, *40*, 10230–10242.
(19) Tairi, A.-P.; Hovius, R.; Pick, H.; Blasey, H.; Bernard, A.; Suprenant, A.; Lundström, K.; Vogel, H. *Biochemistry* **1998**, *37*, 15850–15864.

scheme is shown in part b of Figure 1. First, positively charged poly-L-lysine (PLL) was adsorbed electrostatically on negatively charged quartz (Q). Second, a primary antibody (IgG) was bonded covalently to PLL. Third, IgG then captured a secondary antibody (Abα). Finally, Abα targeted the AF1 region of ERα. Details of the sample preparation are given in the Supporting Information.

Data Capture. A kinetics run usually consisted of fast (seconds) and slow (minutes) events. Slow events were recorded on 2-s long movies taken at 1 min intervals, at 5 Hz frame rate. If spatial averaging was needed, the slide would be translated and 10 or more such movie segments would be taken in prompt succession. To capture fast events, such as the influx of the fluorescent reporter ligands F and their binding with and dissociation from receptors, 30 s movies of the same spot were taken at 5 Hz frame rate. Slight photobleaching could have occurred. Its extent was gauged by comparison with neighboring nonirradiated spots. Movies in TIF format were processed by a MATLAB program in real time. The program summed 10 successive frames and calculated the average brightness over user-defined areas such as the four spots shown in Figure 1c as well as peripheral areas that served as background. The TIRF and FP traces were displayed as the reaction progressed. At the end of a data run, the data traces in text format and the raw TIF file were stored for off-line processing and analysis.

THEORY

Fluorescence Anisotropy. Our kinetics analysis was based on measuring the fluorescence anisotropy of F. The anisotropy parameter A is defined by[10]

$$A = \frac{I_{||} - I_{\perp}}{I_{\text{total}}} \tag{1}$$

where $I_{||}$ and $I_{\perp}$ are the bulk fluorescence intensities of F with polarization parallel and perpendicular to the incident polarization, respectively, and I_{total} is the total fluorescence intensity. Values of A are usually reported in mA, where 1 mA $= 10^{-3}$ A.

If the dipole $\boldsymbol{\mu}$ of F is oriented randomly, I_{total} can be shown to be[10]

$$I_{\text{total}} = I_{||} + 2I_{\perp} \tag{2}$$

and A can be converted to the fraction f of fluorophores bound,[10]

$$f = \frac{A - \underline{A}}{\bar{A} - \underline{A}} \tag{3}$$

In the last equation, $\underline{A}$ is the minimum A value of 100% free F, and $\bar{A}$ is the maximum A value of 100% bound F. We generated 100% free F by two independent methods: (1) by mixing F with a huge excess of a competitor ligand,[20] and (2) by flowing F into a sample channel coated with polyethylene glycol (PEG). We produced 100% bound F again by two independent means. The first was by allowing F to bind to tethered ERα, waiting until equilibrium, and then promptly flushing out all free F and measuring A at that instant. The second was based on mixing F with excess ERα in solution in a PEG-coated channel. All results were found to be consistent and the value of $\underline{A}$ and $\bar{A}$ were about 80 and 320 mA, respectively. We will show in a later section that even for tethered ERα, $\boldsymbol{\mu}$ of bound F was oriented randomly. We could therefore make use of eqs 1−3 to determine $f(t)$ from measured $A(t)$.

Kinetics Modeling. When F was flowed onto tethered ERα, the time rate of change of the surface density of the receptor−F complex $[RF]^{\bullet}$ would be given by[3]

$$\dot{[RF]} = k_{\text{on}}[F]([R]_{\text{total}} - [RF]) - k_{\text{off}}[RF] \tag{4}$$

where $[F]$ was the concentration of free F in solution, $[R]_{\text{total}}$ was the surface density of apo and complexed receptors, and k_{on} and k_{off} were the respective on and off rate constants. Expressing eq 4 in terms of the bound fraction f, we have

$$\dot{f} = k_{\text{on}}(1 - f)(\rho_{\text{total}} - f[F]_{\text{total}}) - k_{\text{off}}f \tag{5}$$

where ρ_{total} was the equivalent volume concentration if all the tethered receptors were dissolved in solution, and $[F]_{\text{total}}$ was the equivalent volume concentration of free and complexed F. By solving eq 5 numerically to best fit the measured $f(t)$, we could determine the three unknowns, ρ_{total} and the two rate constants. We assumed that the mixing of free F in the solution was rapid, so that $[F]$ was homogeneous throughout. This so-called rapid mixing assumption will be justified in the next section.[21]

To model the competition between a dark ligand L and the reporter ligand F, eq 5 had to be modified to two coupled differential equations[17]

$$\dot{f} = k_{\text{on}}(1 - f)(\rho_{\text{total}} - f[F]_{\text{total}} - \tilde{f}[L]_{\text{total}}) - k_{\text{off}}f \tag{6}$$

and

$$\dot{\tilde{f}} = \tilde{k}_{\text{on}}(1 - \tilde{f})(\rho_{\text{total}} - f[F]_{\text{total}} - \tilde{f}[L]_{\text{total}}) - \tilde{k}_{\text{off}}\tilde{f} \tag{7}$$

where variables with tildes were the L analogs of F. In contrast to $[F]_{\text{total}}$, $[L]_{\text{total}}$ could not be measured because L was not fluorescent. Instead, it was determined from dilution ratios based on the known concentration of the stock. For that reason, extra care was taken when preparing and diluting the stock. This was explained in the Supporting Information. The five unknowns, ρ_{total} and the four rate constants in eqs 6 and 7, could be determined by solving the coupled differential equations numerically to best fit the measured $f(t)$.

Rapid Mixing Assumption. To determine if diffusive mixing is rapid enough or not, we can consider the number of F molecules dissociated from unit area of tethered receptors in time τ, where τ is the time for a free F to diffuse half the height h of the sample channel. We use half height because there were tethered receptors on the quartz slide as well as on the coverglass. τ is therefore given by $\tau = (h^2)/(8D)$ where D is the diffusion constant of free F.

(20) We typically mixed 1 nM F with 20 μM of the competitor ligand. The competitor ligand was either E2 or DES. Their dissociation constants were 1.4 nM (see Table 1).

(21) Myszka, D. G.; He, X.; Dembo, M.; Morton, T. A.; Goldstein, B. *Biophys. J.* **1998**, *75*, 583–594.

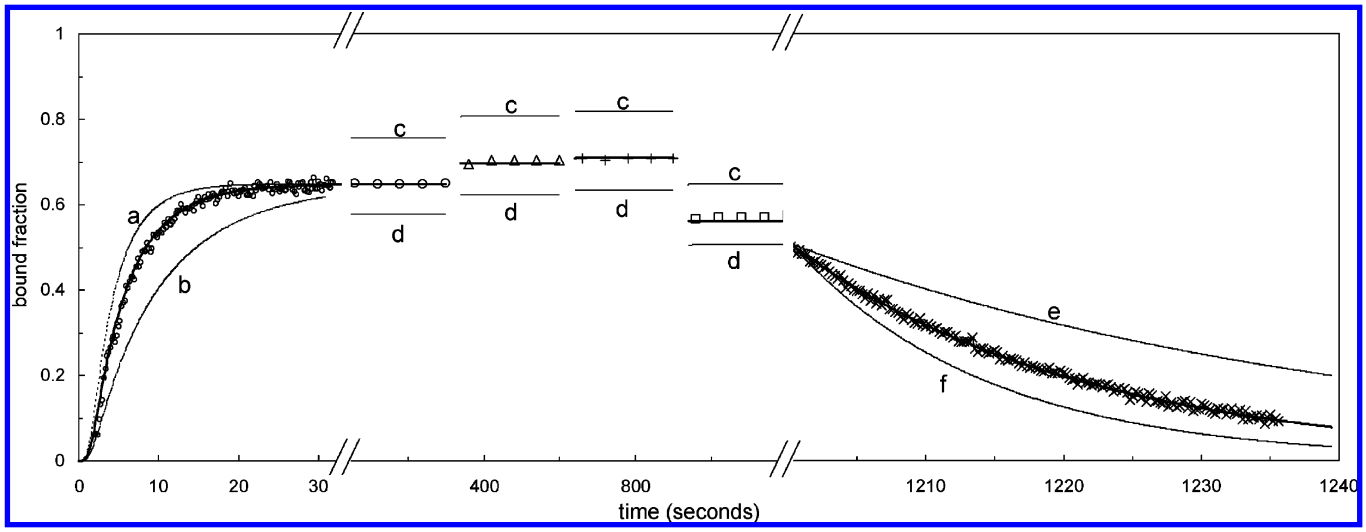

Figure 2. ERα-F binding kinetics. The bound fraction of F as deduced from fluorescence anisotropy was plotted against time as different reagents were injected at various time points. At time $t = 0$, 10 μL of 3 nM F was injected into the sample to replace the initial blank buffer, and the bound fraction was plotted (○). At $t = 300$ s, 15 μL of blank buffer was injected, and the equilibrated bound fraction was shown (△). The last step was repeated at $t = 600$ s, and the equilibrated bound fraction was plotted (+). At $t = 900$ s, 10 μL of 3 nM F was injected and the equilibrated bound fraction was plotted (□). At $t = 1200$ s, 15 μL of 20 μM E2 was injected, and the subsequent dissociation of F from ERα was shown (×). The steady-state signal shown was the average over 10 or more neighboring spots on the sample slide. The standard deviation was about the size of the data symbols. The kinetic rate constants could be determined by best-fitting the experimental data points (bold curves). Misfits were also shown: 50% higher k_{off} (curves labeled d), 50% lower k_{off} (curves labeled c), and both k_{off} and k_{on} 50% higher (curves a and f) and 50% lower (curves b and e).

These freed F molecules are released in a volume of (channel height h) × (unit area). The concentration of released F, relative to the background [F], is thus given by

$$\frac{[F]_{\text{released}}}{[F]_{\text{bkgn}}} = \frac{k_{\text{off}}[R]_{\text{total}}h}{8D[F]_{\text{bkgn}}} \tag{8}$$

If the ratio is much less than 1, mixing is rapid enough.

For association events, one can derive in a similar fashion the criteria for rapid mixing. We also checked the validity of eq 8 by numerically solving the hydrodynamics equations subject to appropriate boundary conditions.[21] The result supported the conclusion drawn from eq 8 (ref 22).

RESULTS AND DISCUSSION

Tether Characterization. Because of the fragility of the estrogen receptor and the stringent requirement of polarization assays,[10,23] we had to experiment with numerous tethering schemes, from simple physisorption, through covalent bonding,[23] to antibody capture.[24] We finally adopted the scheme depicted in Figure 1b. We tested the strength and specificity of the tethering chain. Each link was found to withstand multiple flushes of buffer and reagents. The antibody bridge was shown to be specific: the surface coverage of ERα dropped 18-fold if Abα was absent (Figure S1, Supporting Information). We used a green fluorescent ligand F (Fluormone ES2, Invitrogen) as the reporter in kinetic studies. The binding of F to the channel surface was shown to be extremely specific as well: when 1 nM F was flowed into ERα-coated channels, about 60% were bound; when ERα was absent, the bound fraction dropped to practically zero (Figure S2).

We then enquired if tethering would affect receptor functions. We found that, for our tethered ERα, agonist (17β-estradiol) bound ones recruited 18 times more coactivator than apo ones or antagonist (4-hydroxy-tamoxifen) bound ones (Figure S3), as expected of a functional ERα. We also showed that tethering did not affect the binding kinetics of ERα-F. This will be elaborated later.

We last checked the orientation of the dipole $\boldsymbol{\mu}$ of bound F. During their brief fluorescence lifetime, each $\boldsymbol{\mu}$ was effectively frozen in space. Yet they were shown to be pointing just as randomly, were they bound to receptors in solution or receptors tethered on the quartz slide (Figure S4). The polarization anisotropy A $(=(I_{\parallel} - I_{\perp})/(I_{\text{total}}))$ could thus be readily converted to bound fraction of F.

Binding Kinetics of Green Fluormone F. The binding kinetics of analyte (nonlabeled) ligands was deduced from their displacement of the reporter ligand F. For that reason, the rate constants of F had to be measured first. We did a preliminary study by flowing F onto tethered ERα, waiting until steady state, and displacing the bound F with a high concentration of 4-hydroxy-tamoxifen (4OHT). The result is shown in Figure 1a, where anisotropy A (○) and the TIRF signal (△) are plotted against time. Experimental conditions are described in the figure caption. As can be seen, the two sets of data were very consistent. The anisotropy A, however, could give the absolute bound fraction (eq 3) while TIRF would only give the *relative* population of surface-bound fluorophores. Therefore, in our finalized experimental design, we measured the kinetics by FP. The TIRF data were used for consistency checks.

The results of a typical kinetics run are shown in Figure 2. The experimental conditions are given in the caption. Briefly, at

(22) Kwok, K. C. Measuring Binding Kinetics of Ligands with Tethered Receptors by Fluorescence Polarization Complemented with Total Internal Reflection Fluorescence Microscopy. Ph.D. Thesis, Hong Kong Baptist University, 2010.
(23) Kim, S. H.; Tamrazi, A.; Carlson, K. E.; Daniels, J. R.; Lee, I. Y.; Katzenellenbogen, J. A. *J. Am. Chem. Soc.* **2004**, *126*, 4754–4755.
(24) Wingren, C.; Borrebaeck, C. A. K. *OMICS* **2006**, *10*, 411–427.

Table 1. Rate Constants, Dissociation Constants, and Relative Binding Affinities (RBA) of ERα−Ligand Interactions

	k_{on} (10^5 M^{-1} s^{-1})		k_{off} (10^{-3} s^{-1})		$K_L = k_{off}/k_{on}$ (nM)		RBA		
ligand	this work	Rich 2002[a]	this work	Rich 2002	this work	Rich 2002	this work	Rich 2002	hERα-FP[b]
Agonist									
green F	570 (100)		30 (5)		0.5 (1)		270 (60)		140 (70)
E2	11 (3)	13 (6)	1.5 (4)	1.2 (2)	1.4 (5)	0.9 (4)	100	100	100
DES	10 (1)	60 (7)	1.5 (3)	0.05 (2)	1.4 (3)	0.009 (3)	100 (20)	1.0 (3) × 10^4	120 (30)
genistein	0.26 (8)		2.3 (5)		90 (30)		1.5 (6)		6 (9)
Antagonist									
raloxifene	3.3 (5)		1.3 (5)		4 (2)		35 (17)		29 (30)[c]
4OHT	2.4 (9)	0.023 (1)	1.6 (4)	0.041 (1)	7 (3)	18 (1)	21 (9)	5.0 (3)	17 (8)
tamoxifen	1.0 (3)	0.045 (1)	1.73 (6)	1.0 (1)	18 (6)	220 (20)	8 (3)	0.41 (4)	4 (3)

[a] Rich 2002 (ref 8). [b] RBA values of human full length ERα measured by FP, as reported in the literature (refs 2 and 25–27, and vendor). [c] RBA values of human full length ERα measured by FP and radio-assays, as reported in the literature (refs 27–30).

$t = 0$, F was injected into a sample channel of tethered ERα. Flow was promptly ceased, and binding occurred in a static cell environment during the next 300 s. Blank buffer or F was then injected a few more times, when new steady states were generated each time. At t = 1200 s, excess 17β-estradiol was injected to completely displace all bound F.

With reference to Figure 2, the simulation of the empirical data was done in four steps. First, the off-rate was easily found because the decay beyond 1200 s was due solely to dissociation of F. Rebinding was prevented by excess E2. Second, the receptor coverage and the equilibrium dissociation constant K_D (= k_{off}/k_{on}) were determined by fitting the four steady-state bound fractions between 100 and 1000 s. Four steady-state values overdetermined the two unknowns to allow parameter optimization and consistency checks. Third, we used the determined rate constants and receptor coverage to generate the association curve. The transient influx of F near $t = 0$, as measured by $I_{total}(t)$, was taken into account in the simulation (Figure S8). As there were no free parameters, the excellent match to the experimental data lent confidence to the model. Four, we finally optimized the three parameters to best fit all data points.

The best fit is shown in Figure 2 (bold solid curves), which yielded both the on and off rates. The sensitivity of the fit to parameter values was also examined. A 50% higher k_{off} visibly underestimated the equilibrated bound fractions (light curves labeled d) while a 50% lower k_{off} overestimated them (light curves labeled c). If both k_{off} and k_{on} were 50% higher, the F signal would increase too fast (light curve a) and decay too soon (light curve f). The exact opposite would occur if both rate constants were 50% lower than the best-fit values (light curves b and e).

Multiple sets of rate constants were found from fitting more than 10 sets of data. To test reproducibility, these data sets were captured using different sample cells in experiments performed in different sessions, even on different days. The averaged rate constants are given in Table 1 (first row). The standard deviations are shown as uncertainties. As can be seen, the uncertainties were within 20%.

Rate constants were also measured in PEG-coated channels when receptor−ligand interactions occurred in solution. The on and off rates were found by FP to be 6.8×10^7 M^{-1} s^{-1} and 2.5×10^{-2} s^{-1}, respectively. The relative uncertainty was about 20%. Their agreement with those of tethered ERα, to within experimental error (see Table 1), indicated that tethering did not affect the binding kinetics.

From the best fit, the receptor coverage was found to be about 30 molecules μm^{-2}. At this low coverage, the perturbation in local [F] due to binding with or dissociation from tethered ERα was less than 2% (eq 8). This justified the assumption of rapid mixing.

Binding Kinetics of Nonfluorescent Ligands. The binding kinetics of a dark ligand L was determined by its competitive displacement of the reporter F. The result of a typical experiment is shown in Figure 3 when the dark ligand genistein was used. The measured bound fractions are plotted as data points (○, △, ×, and □). The experimental conditions are given in the caption.

With reference to Figure 3, the experimental data were fitted as follows. First, the rate constants of ERα-F interaction and the receptor coverage were found by fitting the initial 600 s of data. Values of the rate constants should be the same as those gotten previously (see Table 1, first row). Once this consistency was checked, the final dissociation phase was fitted in two steps to determine the rate constants of L. In step one, the steady-state bound fraction at t = 1200 s was fitted to give $(\tilde{k}_{off})/(\tilde{k}_{on})$. In step two, the shape of the dissociation curve (600 s < t < 1000 s) was fitted to give $\tilde{k}_{off}$ and $\tilde{k}_{on}$.

The best fit is shown in Figure 3 (bold solid curves). The on and off rates $\tilde{k}_{on}$ and $\tilde{k}_{off}$ of L were hence determined. Tolerance in the fitted values is again illustrated in the figure.

Multiple sets of rate constants of genistein were gotten from fitting three sets of data. These data sets were again captured in different sessions. The averaged rate constants are given in Table 1. The standard deviations are shown as uncertainties. Besides genistein, five other standard ligands of ERα were studied. They were 17β-estradiol (E2), diethylstilbestrol (DES), raloxifene,

(25) Ohno, K.; Suzuki, S.; Fukushima, T.; Maeda, M.; Santa, T.; Imai, K. *Analyst* **2003**, *128*, 1091–1096.
(26) Mueller, S. O.; Simon, S.; Chae, K.; Metzler, M.; Korach, K. S. *Toxicol. Sci.* **2004**, *80*, 14–25.
(27) Clegg, N. J.; Paruthiyil, S.; Leitman, D. C.; Scanlan, T. S. *J. Med. Chem.* **2005**, *48*, 5989–6003.
(28) Grese, T. A. *Proc. Natl. Acad. Sci. U.S.A.* **1997**, *94*, 14105–14110.
(29) Wijayaratne, A. L.; Nagel, S. C.; Paige, L. A.; Christensen, D. J.; Norris, J. D.; Fowlkes, D. M.; McDonnell, D. P. *Endocrinology* **1999**, *140*, 5828–5840.
(30) Kuiper, G. G. J. M.; Lemmen, J. G.; Carlsson, B.; Corton, J. C.; Safe, S. H.; van der Saag, P. T.; van der Burg, B.; Gustafsson, J.-A. *Endocrinology* **1998**, *139*, 4252–4263.

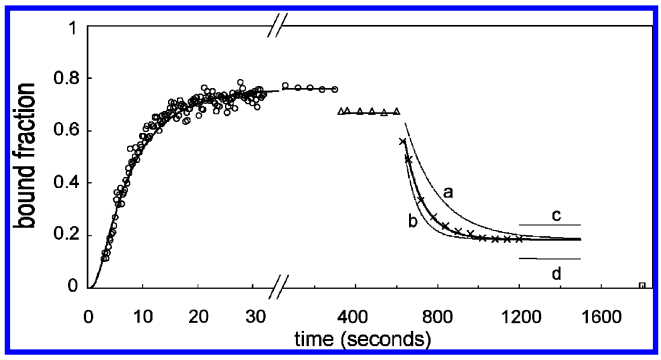

Figure 3. ERα-genistein binding kinetics. The bound fraction of F as deduced from anisotropy *A* was plotted against time while different reagents were injected at various time points. At $t = 0$, 10 μL of 1 nM F was flowed into the sample cell (○). At $t = 300$ s, another 10 μL of 1 nM F was flowed in, and the equilibrated bound fraction was shown (△). At $t = 600$ s, 15 μL of 1 μM genistein was flowed in, and the subsequent dissociation of F from ERα was shown (×). At $t = 1200$ s, 15 μL of 10 μM E2 was flowed in to generate the baseline (□). The error bar of the steady-state signal was about the size of the data symbols. For the data shown, photobleaching was found to be negligible. The rate constants of the ERα-F binding kinetics could be determined by best-fitting the experimental data points for $t < 600$ s (bold curves). For the ERα-genistein complex, the rate constants could be determined by best-fitting the remaining experimental data points (bold decay curve). Misfits were also shown: 50% higher k_{off} (curve labeled d), 50% lower k_{off} (curve c), and both k_{off} and k_{on} 50% higher (curve b) and 50% lower (curve a).

4-hydroxytamoxifen (4OHT), and tamoxifen. They were chosen because they were standard ligands of ERα or approved antiestrogen drugs. Their measured rate constants are listed in Table 1. The uncertainties were based on three or more data sets. They were mostly within 30%.

As far as we know, the values of the kinetic rate constants listed in Table 1 were known only for the first time. To date, none were reported in the literature. The nearest that we could find were rate constants measured by Rich et al. 2002 (ref 8), but they used the ligand binding domain (LBD) of ERα while we used full length receptors. Their results are also given in Table 1 for easy comparison. As could be seen, except for E2, the rate constants differed very significantly.

Later on, we will comment on the discrepancy. Here, it is useful to point out that equilibrium binding affinity data were available in the literature. They were usually reported in terms of relative binding affinity (RBA) of ERα-L relative to ERα-E2.[2] It could be computed once the dissociation constant K_L was known (see Supporting Information). The computed values are listed in Table 1.

RBA values were reported by numerous other groups. Among them, we selected those studies when full length human ERα was assayed by fluorescence polarization (hERα-FP).[2,25–27] We averaged the reported values and computed their standard deviations. The results are also tabulated in Table 1 for easy comparison. As could be seen, our RBA values were consistent with the reported ones. For the case of raloxifene, only one hERα-FP result was available.[27] We therefore quoted the results of radio-assays performed on full length human ERα as well.[28–30]

We could also compute the RBA values based on the results of Rich in 2002 (ref 8). These are shown in Table 1. They were very different from the other reported values. Rich in 2002 used SPR to assay the binding of ERα(LBD) with its ligands while all the others used FP to study full length ERα. That might explain the difference.

All the known ERα ligands that we have studied did bind to ERα and competed with F for ERα. In other words, all the positive results that we saw were true positives. We also checked for false negatives. We tested dexamethasone and testosterone which were known to be non ERα ligands. No binding was detected (Figure S5).

From Table 1, interesting pharmacological implications could be drawn. The relative binding affinities of the ligands ranged from 1.5 to 100, but the off-rates only varied from 1.3×10^{-3} s^{-1} to 2.3×10^{-3} s^{-1} (see Table 1). If off-rates correlated better with *in vivo* downstream effects than binding affinities,[4] we would expect similar potency for these ligands. This was indeed the case for tamoxifen and raloxifene. From Table 1, raloxifene would bind 4 times stronger than tamoxifen, but the two drugs were shown to reduce breast cancer risk by about the same factor when they were administered at comparable dosage.[31] Admittedly, a 4-fold difference in affinity may be too small to be clinically significant, but it illustrates how our technique can be applied to study the correlation between off-rate and drug potency.

Screening Ginsenosides for Binding with Nuclear Receptors. As mentioned, our FP-TIRF method could be used to screen potential ligands of the tethered receptor. We screened a total of 11 ginsenosides for binding with tethered ERα. They were Rb1(S), 20(R)-Rg3, 20(S)-Rg3, 20(R)-Rh2, 20(S)-Rh2, Rg1, Re, PPT, PPD, CK, and F1. They were chosen because of their steroidlike properties.[32] Each ginsenoside at high concentration (10−50 μM) was flowed onto tethered ERα-F complex, and the displacement of F was monitored. All 11 ginsenosides were screened 3 times. No measurable binding of any of the ginsenosides with ERα was observed (Figure S6). The null results were double-checked using fluorescence polarization assays in solution.[22] The two results agreed.

Using the FP-TIRF system, we screened the same 11 ginsenosides for binding with surface-immobilized PPARγ (LBD). PPARγ was chosen because it was recently implicated in the antidiabetic effects of ginsenosides.[33,34] To immobilize this receptor, we found that it could be physisorbed firmly on PLL-coated surfaces. The tethering procedure was therefore simplified. Binding was measured by TIRF. Only two ginsenosides, Rb1(S) and 20(S)-Rg3, showed measurable binding to PPARγ (Figure S7). We then double-checked the reliability of the screening results by repeating the experiment but with the PPARγ (LBD) captured by a surface-immobilized antibody specific for the receptor.[22] This time, we used FP to measure the binding. Results are shown in Figure 4. Clearly, the same conclusion could be drawn. Both the positive and negative results were double-checked using fluorescence polarization assays in solution.[22] The two results agreed.

(31) STAR Results: Raloxifene as Effective as Tamoxifen, Better Safety Profile. NCI Cancer Bulletin; National Cancer Institute, April 18, 2006; *Vol. 3* (16).
(32) Furukawa, T.; Bai, C. X.; Kaihara, A.; Ozaki, E.; Kawano, T.; Nakay, Y.; Awais, M.; Sato, M.; Umezawa, Y.; Kurokawa, J. *Mol. Pharmacol.* **2006**, *70*, 1916–1924.
(33) Shang, W.; Yang, Y.; Zhou, L.; Jiang, B.; Jin, H.; Chen, M. *J. Endocrinol.* **2008**, *198*, 561–569.
(34) Hwang, J. T.; Lee, M. S.; Kim, H. J.; Sung, M. J.; Kim, H. Y.; Kim, M. S.; Kwon, D. Y. *Phytother. Res.* **2009**, *23*, 262–266.

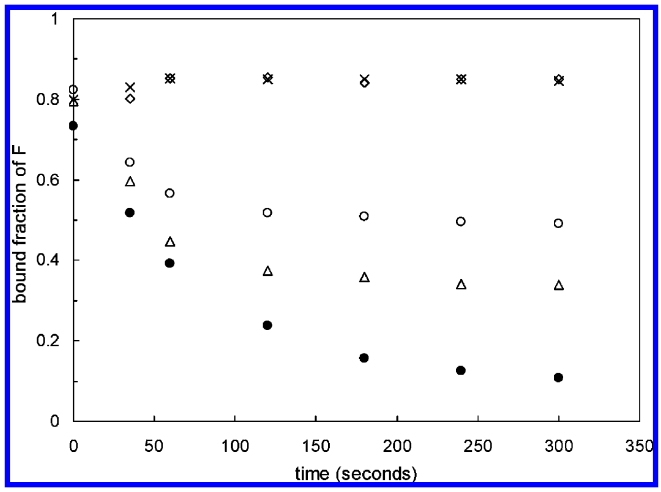

Figure 4. Screening ginsenosides for binding with antibody-captured PPARγ. Tethered PPARγ was first complexed with F. A 10 μM sample of a ginsenoside was injected into the sample channel at time $t = 0$, and fluorescence anisotropy was measured for the next 300 s and converted to bound F fraction. The cell was refreshed by flushing with blank buffer. The injection−wash cycle was repeated with a new ginsenoside each time. Results of three ginsenosides were shown: Rb1 (△), 20(S)-Rg3 (○), and 20(R)-Rg3 (×). Blank buffer was used as negative control (◇). As positive control, a PPARγ standard ligand GW9662 at 10 μM was injected in the last round to determine the minimum anisotropy (●).

The therapeutic effects of ginsenosides on diabetic mice had since been investigated by our collaborators, and very interesting results that corroborated strongly with our findings were observed.[35]

Our fast screen results may also help to relate the ligand structure with its function. For instance, the absence of the aromatic A-ring might be a possible explanation for nonbinding with ERα,[36] and the orientation of the hydroxyl group on the chiral carbon (C-20) and the sugar moiety at C-3 might be decisive for binding with PPARγ.

CONCLUSION

We reported a method to measure the binding kinetics of tethered nuclear receptors with their specific ligands. It was based on FP anisotropy of a fluorescent reporter ligand that competed with the analyte ligands. The same apparatus also measured the TIRF signal of surface-bound reporter ligands.

Our method gave reliable results based on straightforward data analysis. The data interpretation was clean because the tethering scheme preserved the random pointing of the reporter dipole. This simplified the data analysis. At the same time, the sensitive detection tolerated low receptor coverage which in turn justified position-independent kinetics modeling. When the receptor coverage was high, as in the case of SPR, elaborate models would be needed.[21] The data accuracy was checked by the consistency of the FP and the TIRF signals. The model validity was ensured by the satisfactory fit to empirical data. The very good agreement between our measured affinities and those reported in the literature speaks for the reliability of our results.

Our method also saved money and time. The setup was inexpensive: the entire apparatus cost less than 20 000 USD if the electron-multiplied CCD (emCCD) was replaced with photomultiplier tubes. An emCCD was used to locate areas-of-interest on the image. For mature setups, however, this will not be necessary. The recurrent cost was low: our sample cell could be easily fabricated and disassembled for cleaning and recycling, and only tens of femtomoles of the reporter ligand were needed as opposed to the picomoles required in conventional FP assays. The measurement was fast: the screening of 11 ginsenosides took less than 2 h, and the rate constants for an analyte ligand could be determined in less than 30 min.

Yet more importantly, we believe our method is presently the only nonradioisotope assay that can reliably measure the kinetic rate constants of receptors interacting with small (10^1−10^2 D) ligands. Realizing that receptor−ligand interaction is the primary step in chemical signaling on the one hand, and fluorescent ligands are becoming readily available on the other,[37] the application horizon is vast.

ACKNOWLEDGMENT

We thank Professors R.N.S. Wong and Y.K. Cheng of Hong Kong Baptist University for their helpful suggestions. We thank Professor R.N.S. Wong and his group for carrying out the binding studies of ginsenosides with ERα by FP in solution, and Professor Yu Huang of Chinese University of Hong Kong for communicating their experimental results of the therapeutic effects of ginsenosides on diabetic mice prior to publication. This work was supported by the General Research Fund and the Collaborative Research Fund of the Research Grants Council of Hong Kong, and the Faculty Research Grants of Hong Kong Baptist University.

SUPPORTING INFORMATION AVAILABLE

Additional expeimental details, explanations of calculations, and figures. This material is available free of charge via the Internet at http://pubs.acs.org.

Received for review January 26, 2010. Accepted March 31, 2010.

AC1002245

(35) Huang, Y. Private communication.

(36) Baker, M. E.; Chang, D. J. *Biochem. Biophys. Res. Commun.* **2009**, *386*, 516–520.

(37) Fluorescent ligands for AR, ERα, ERβ, GR, PPARα, PPARδ, PPARγ, PR, PXR (SXR), and VDR are available from Invitrogen.